analytical chemistry

Article

Cite This: *Anal. Chem.* 2019, 91, 4883−4888

pubs.acs.org/ac

Ultrasensitive Electrochemiluminescence Biosensor for Speedy Detection of microRNA Based on a DNA Rolling Machine and Target Recycling

Ziqi Xu, Yuanyuan Chang, Yaqin Chai, Haijun Wang,* and Ruo Yuan*

Key Laboratory of Luminescent and Real-Time Analytical Chemistry, Ministry of Education, College of Chemistry and Chemical Engineering, Southwest University, Chongqing 400715, People's Republic of China

Supporting Information

ABSTRACT: Intelligent DNA walking machines have become a great hot spot in biosensing, but the walking efficiency of DNA walking machines was still limited due to the low local concentration of substance DNA and the derail of leg DNA. Herein, a Zn^{2+}-driven DNA rolling machine was proposed to overcome the above shortages and applied as a electrochemiluminescence (ECL) biosensor for speedy ultrasensitive detection of microRNA-21. First, the original DNA rolling machine was synthesized by numbers of leg DNA modified on Au nanoparticle which matched with the high concentration of track DNA on the sensing platform and could roll efficiently through Zn^{2+} driving. By this way the DNA rolling machine not only increased the local concentration of leg DNA and track DNA to improve walking efficiency but also changed the motion mode from step-by-step walking to high-speed rolling, weakening the derailment of leg DNA and shortening the moving time. Second, target-induced recycling and acid dissolution could convert a finite amount of target microRNA into a large amount of Zn^{2+}, which greatly improved the sensitivity of biosensor and overcame the drawbacks of enzyme cleavage or polymerization in common nucleic acid amplification methods. Lastly, the obtained Zn^{2+} was employed to drive the DNA rolling machine through specific sites recognizing and track DNA cutting to remove a quencher of ferrocene, recovering ECL emission of CdS:Mn QDs for microRNA-21 detection with a detection limit of 0.28 fM. Besides, the biosensor was successfully applied in microRNA-21 analysis from human cancer cell lysates, offered a controllable and ultrasensitive strategy for speedy detection of microRNA, and revealed a new avenue for clinical analyses.

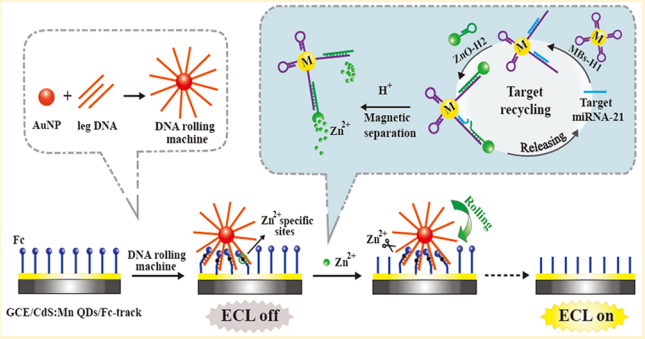

INTRODUCTION

DNA walking machines have been widely used in biosensing for their efficient self-assembly nanostructures, cargo handling capacities, and diverting biomimetic phenomena, improving the detection sensitivity and showing great promise in biological applications.[1−3] However, the walking efficiency of conventional DNA walking machines was unsatisfactory due to its low local concentration of leg or track DNA and the limited movement space for leg DNA.[4,5] According to reports[6,7] increasing the concentration of substance DNA was helpful for the interlocking force of legs and tracks, which further improved the walking efficiency and velocity. For example, Milan N. Stojanovic's group studied a DNAzyme-fueled DNA walking machine, and the walking velocity increased correspondingly as the number of legs increased.[8] Recently, a newly reported three-dimensional DNA walking machine assembled a large number of track DNA on the gold nanoparticles (AuNPs) to increase the local concentration of track DNA for improving the walking efficiency to a degree.[9] Unfortunately, the unsatisfactory walking efficiency caused by the low local concentration of substance DNA was still a problem, and another difficult problem that leg DNA was inclined to derail the track during walking also notably restricted the walking efficiency. Therefore, it is extremely challenging to solve these problems.

Rapid analysis, which means a shorter reaction time and lower waiting time, is of great significance in diagnostics and therapeutics.[10,11] However, since the driving force of the DNA walking machine comes from the free energy of leg DNA combined with a next track DNA followed by DNA enzyme hydrolyzing of the fuel chain, this free energy unavoidably causes Brownian motion to deviate from consumed substrate according to Burning Bridge Ratchet, obstructing the walking efficiency and resulting in an unsatisfied moving time, which undoubtedly is the inherent deficiency of the DNA walking machine.[12−14] Here, a Zn^{2+}-driven DNA rolling machine was proposed to overcome those problems by increasing the concentration of both leg DNA and track DNA to enhance the

Received: February 8, 2019
Accepted: March 12, 2019
Published: March 12, 2019

DOI: 10.1021/acs.analchem.9b00728
Anal. Chem. 2019, 91, 4883−4888

Scheme 1. Fabrication Process of the ECL Biosensor Based on a Zn^{2+}-Driven DNA Rolling Machine for Speedy Detection of miRNA-21 (A), Preparation of DNA Rolling Machine (B), and Conversion from Target miRNA to Zn^{2+}(C)

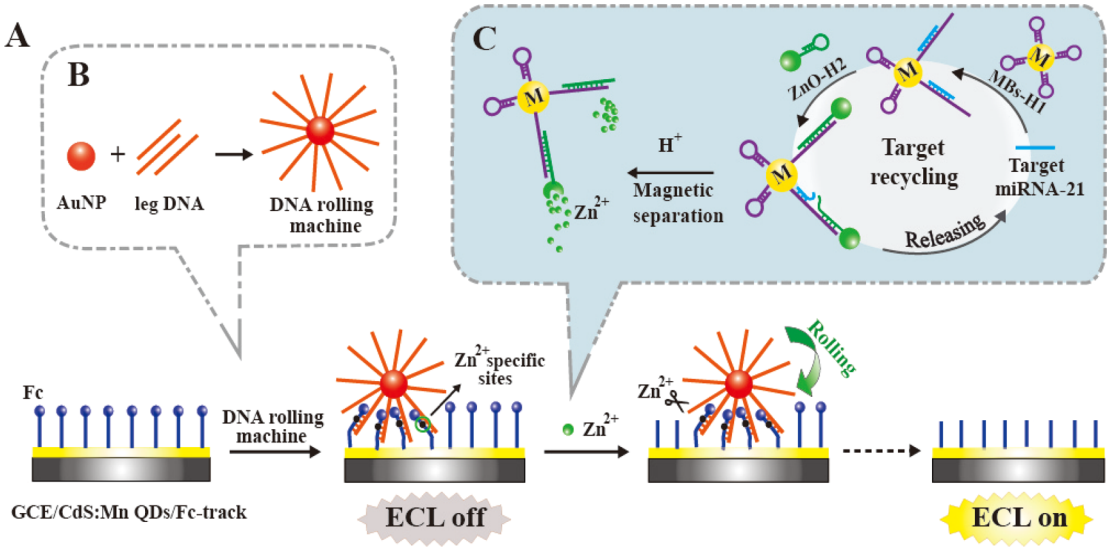

walking efficiency and changing the motion mode from step-by-step walking to high-speed rolling to reduce the derailment of leg DNA. As a result, the proposed DNA rolling machine would possess excellent signal amplification capability that provided good application in ultrasensitive and speedy electrochemiluminescence (ECL) analysis.

According to the above points, we proposed an electrochemiluminescence biosensor for speedy ultrasensitive detection of microRNA-21 (miRNA-21), which is high expression in serum or expiratory condensate of lung cancer patients. As seen in Scheme 1A, CdS:Mn quantum dots (QDs) were employed on the electrode surface as substrate luminescent to obtain an initial ECL signal; then the ferrocene (Fc) was assembled on track DNA as the quencher to weaken the ECL emission, resulting in a low ECL signal. Subsequently, the DNA rolling machine was constructed by AuNP modified with numbers of DNA legs (seen in Scheme 1B), which matched with the Fc-labeled track DNA on the sensing platform to obtain recognition sites of Zn^{2+}. Then target-induced recycling and acid dissolution converted a small quantity of target miRNA-21 into a large amount of Zn^{2+} (seen in Scheme 1C), which greatly improved the sensitivity of the biosensor and overcame the drawbacks of enzyme cleavage or polymerization such as complex operation and false positive signals in conventional target amplification techniques.[15,16] Notably, the obtained Zn^{2+} fueled high-speed rolling of the DNA rolling machine with a short reaction time for only 20 min and cut off the Fc-labeled track DNA to restore the ECL emission of CdS:Mn QDs, achieving sensitive detection of miRNA-21 with a detection limit of 0.28 fM. In summary, the method based on the proposed DNA rolling machine not only raised the efficiency and velocity for speedy miRNA detection but also unveiled a great potential application especially in biomarker assay and early cancer diagnoses.

EXPERIMENTAL SECTION

Preparation of DNA Rolling Machine. First, AuNPs were synthesized according to ref 17. Briefly, 30 mL of $HAuCl_4$ (0.25 mM) containing 1 mL of ice cold $NaBH_4$ (0.1 M) was stirred until it turned orange red, and the AuNPs were obtained through centrifugation. Next, a mixture containing 100 μL of leg DNA (2.5 μM), 100 μL of NaCl (0.1 M), and 500 μL of the above AuNPs was stirred for 16 h. Finally, the DNA rolling machine containing a large number of legs was obtained after separation and abstersion and dispersed in 500 μL of Tris-HCl under 4 °C for further use.

Preparation of the miRNA-Mediated Zn^{2+}. The preparation process of the target miRNA-mediated Zn^{2+} were as follows. First, 20 μL of target miRNA-21 was added into a mixture containing 10 μL of MBs-H1 and 10 μL of ZnO-H2 to open the hairpin structure of H1 and induce chain displacement of H2. By hybridization of H1 and H2, the target miRNA-21 was released and participated in opening the next hairpin H1. Thus, the miRNA-21 was recycled to generate a lot of MBs−H1−H2−ZnO, which was acquired by magnetic separating and washing. Then 20 μL of Tris-HCl containing HCl (pH = 5.5) was added to dissolve ZnO into Zn^{2+}, and the Zn^{2+} released into the solution was separated from the MBs−H1−H2−ZnO and stored at 4 °C for later use.

Fabrication of the ECL Biosensor. For fabricating the ECL biosensor, a cleaned glassy carbon electrode (GCE) was first incubated with 20 μL of CdS:Mn QDs at room temperature overnight. Then 20 μL of EDC (40 mM) was incubated on the electrode for 15 min to activate the carboxylic groups of CdS:Mn QDs which further cross-linked with the activated amino group of Fc-labeled track (20 μL, 2.5 μM) for 1 h; thus, the ECL emission of CdS:Mn QDs was quenched by Fc (ECL off). Later, 20 μL of a mixture of DNA rolling machine and target miRNA-mediated Zn^{2+} was added on the sensing platform, obtaining a high concentration of leg-track double-strand DNA with a lot of recognition sites of Zn^{2+}. Thus, the DNA rolling machine could speedily roll with Zn^{2+} cutting off-track DNA and releasing leg DNA on the basis of a gears and wheels mechanism. In this case Fc was removed, leading towas recovery of CdS:Mn QDs ECL emission for miRNA detection (ECL on).

Experimental Procedure. For detection, biosensors with different concentrations of miRNA-21 were placed in an ECL detector containing PBS (2 mL, pH = 7.4) with 0.05 M $S_2O_8^{2-}$. The potential scanning range was from 0 to −1.2 V,

DOI: 10.1021/acs.analchem.9b00728
Anal. Chem. 2019, 91, 4883−4888

and the photomultiplier tube was 800 V. With the increase of miRNA-21 concentration, the target-induced Zn^{2+} also increased to drive the DNA rolling machine, leading to enhanced ECL signal. Thus, the change of ECL signal directly reflects the change of miRNA-21 concentration.

RESULTS AND DISCUSSIONS

ECL and EIS Characterization of the Biosensor. ECL was employed to prove the "off−on" switch of the biosensor. As shown in Figure 1A, a large amount of Fc-labeled track DNA was introduced on the sensing platform to quench the ECL emission of CdS:Mn QDs (curve a, "off" state). Then, by target-induced recycling and acid dissolving, a small amount of target miRNA was converted into a large amount of Zn^{2+}, which later induced high-speed rolling of the DNA rolling machine and cut off the Fc-labeled track DNA to restore ECL emission of CdS:Mn QDs (curve b, "on" state), achieving miRNA-21 detection. Also, the above results showed the feasible "off−on" switch of the method. Besides, electrochemical impedance spectroscopy (EIS) characterization was utilized to investigate the interfacial process of the biosensor. As seen in Figure 1B, curve a shows the electron transfer resistance (R_{et}) of bare GCE. Later, an increasing R_{et} could be observed after modification of CdS:Mn QDs due to its intrinsic semiconductive property (curve b). Then when the Fc-labeled track DNA was introduced, a weakened R_{et} was obtained owing to the excellent electronic conductivity of Fc (curve c). Finally, the addition of a DNA rolling machine and target-induced Zn^{2+} led a significantly increased R_{et}, suggesting Zn^{2+} fueled the DNA rolling machine and cut off the Fc-labeled track DNA to remove Fc (curve d). Thus, an increased R_{et} could be observed owing to dismissing of Fc with excellent electronic conductivity. Conforming to expectations, all of the results indicated the satisfactory fabrication of the biosensor.

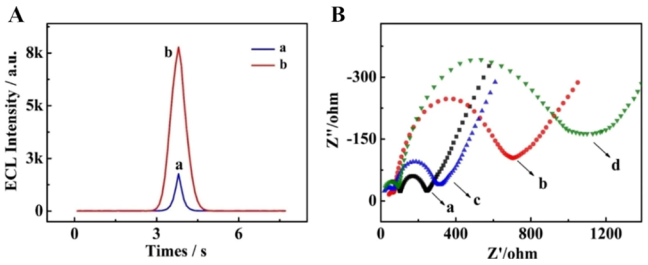

Figure 1. (A) ECL curves of the stepwise-modified electrode in 2 mL of PBS solution (pH = 7.4) containing 0.05 M $S_2O_8^{2-}$: (a) GCE/CdS:Mn QDs/Fc-track and (b) GCE/CdS:Mn QDs/Fc-track incubated with DNA rolling machine and Zn^{2+}. (B) EIS diagram of the biosensor assembly process: (a) GCE, (b) GCE/CdS:Mn QDs, (c) GCE/CdS:Mn QDs/Fc-track, and (d) GCE/CdS:Mn QDs/Fc-track/DNA rolling machine and Zn^{2+}.

Condition Optimization. In order to optimize the detection conditions for improving the sensitivity and velocity of the biosensor, the ratio between leg DNA and track DNA, the pH of ZnO dissolution, and the rolling time of the Zn^{2+}-driven DNA roller were studied. First, the ratio between leg DNA and track DNA which was closely related to the rolling efficiency of the DNA rolling machine was optimized. As shown in Figure 2A, as the proportion of leg DNA and track DNA changed from 1:0.5 to 1:50, the ECL signal increased correspondingly and reached a platform at 1:20. Thus, the ratio of 1:20 was chosen as the optimum ratio of leg DNA and track DNA. Moreover, the pH in this system not only affected the activity of DNA but also led the dissolution of ZnO, which was highly correlated with the sensitivity of the biosensor and should be studied. Also, the results are shown in Figure 2B, the biosensor achieved the highest ECL emission at pH 5.5, which was selected as the appropriate experimental condition. For speedy detection, the rolling time of a Zn^{2+}-driven DNA rolling machine was the decisive factor. As seen in Figure 2C, the rolling time from 5 to 40 min led an increasing ECL signal, and the maximum platform could be observed at 20 min. Hence, the rolling time of the Zn^{2+}-driven DNA rolling machine was chosen as 20 min for the most suitable condition in this system.

Comparison with DNA Walking Machine and DNA Rolling Machine. For a more intuitive confirmation of the walking efficiency and moving velocity, the ECL signal comparison was performed between a traditional DNA walking machine and a DNA rolling machine. As seen in Figure 3A, in the DNA walking machine, a number of track DNA was assembled on the sensing platform and then leg DNA paired with track DNA to obtain recognized sites for Zn^{2+}. After being cleaved by Zn^{2+}, leg DNA was released, which could pair with another track DNA to realize the step-by-step walking on the sensing platform. In this process experimental conditions including the concentration of track DNA and leg DNA employed in the DNA walking machine were equal to that of the DNA rolling machine. The results are shown as Figure 3B; the electrode incubated with a DNA rolling machine obviously showed a faster and stronger ECL response (red line). However, the electrode modified with the same concentration of track DNA and leg DNA to obtain a common DNA walking

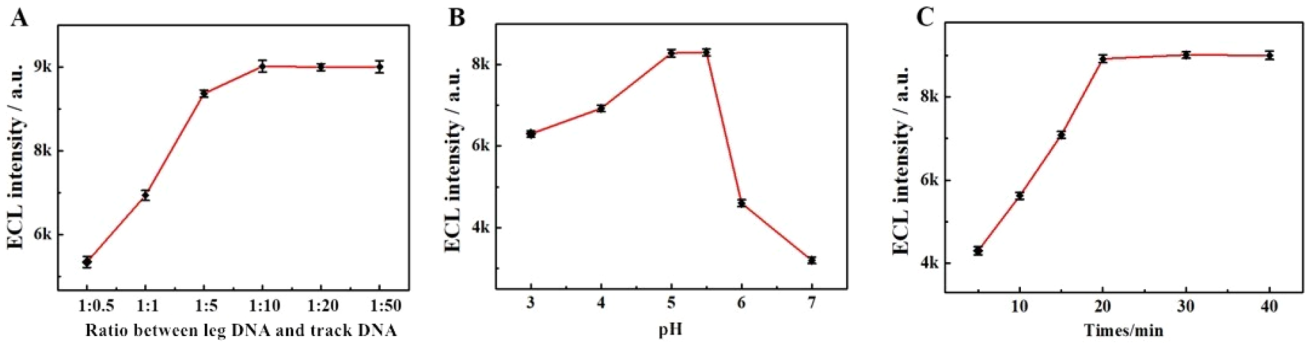

Figure 2. (A) ECL effect of the ratio between leg DNA and track DNA. (B) pH optimization of ZnO dissolution. (C) Rolling time of the Zn^{2+}-driven DNA rolling machine.

DOI: 10.1021/acs.analchem.9b00728
Anal. Chem. 2019, 91, 4883−4888

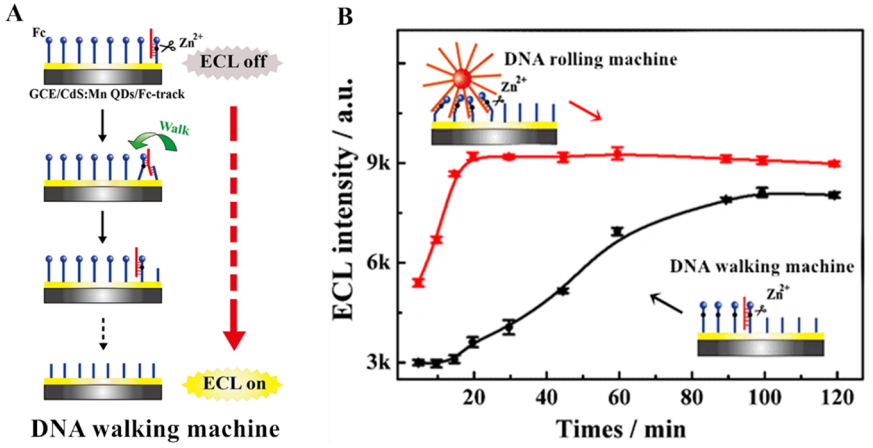

Figure 3. (A) Walking diagram of the DNA walking machine and (B) ECL response of the biosensor for detecting miRNA-21 (1 pM) incubated with DNA rolling machine (red line) and DNA walking machine (black line), respectively.

machine showed a low ECL emission with slow growth (black line). The results are consistent with our expectation, indicating that the walking mode was not as efficient and fast as the rolling mode. In particular, the biosensor on account of the DNA rolling machine needed only 20 min to full reaction, while a conventional DNA walking machine needed at least 100 min, which showed great potential of the DNA rolling machine in rapid ECL detection and other fields such as rapid drug release and biological analysis.

Detection of Target miRNA-21. For exploring the sensitivity analysis of this method the designed biosensor was exploited to detect miRNA-21 with a series of concentrations under the optimum conditions. As shown in Figure 4, with an incremental concentration of miRNA-21 ranging from 1 fM to 100 pM, the corresponding ECL signal increased gradually. Also, the inset shows it linearly responded to the logarithm of miRNA-21 concentrations with a regression equation of I = 9365.81 + 1277.35 lg c (I stands for the ECL intensity and c stands for the concentration of miRNA-21) and squared correlation coefficient of R^2 = 0.9976

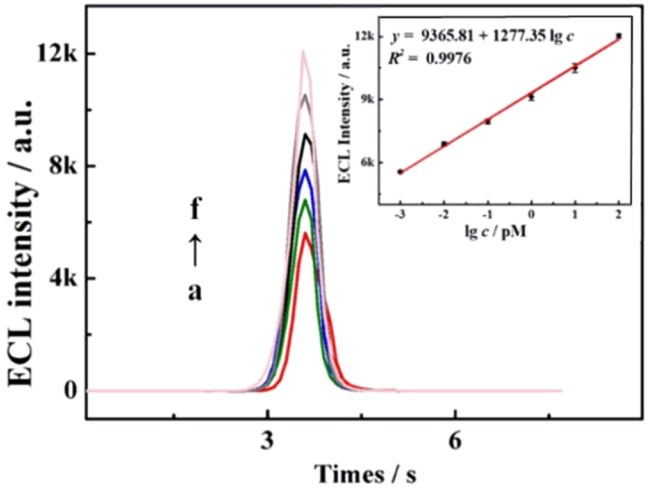

Figure 4. ECL response of the designed biosensor in the presence of miRNA-21: (a) 1 fM, (b) 10 fM, (c) 100 fM, (d) 1 pM, (e) 10 pM, and (f) 100 pM. (Inset) Calibration plot of the miRNA-21 analysis. ECL measurement was carried out in 2 mL of PBS (pH = 7.4) contained with 0.05 M $S_2O_8^{2-}$ (scan range from 0 to −1.2 V vs Ag/AgCl, photomultiplier tube at 800 V).

with an estimated detection limit of 0.28 fM (LOD = $3S_B/m$, where m is the slope of the corresponding calibration curve and S_B is the standard deviation of the blank).[18−20] In addition, the proposed biosensor projected a higher sensitivity and lower detection limit compared with some existing analysis methods (Table S2).

Performance of the Biosensor. As the biosensor's important parameter, the stability was estimated by testing the ECL emission of miRNA-21 in a cyclic potential scan for 16 cycles. According to Figure 5A, the biosensor presented a preeminent stable ECL emission with a relative standard deviation (RSD) of 1.79%. Moreover, the proposed biosensor also presented a wonderful selectivity by evaluating target miRNA-21 with other interfering agents such as miRNA-141 and miRNA-155. As described in Figure 5B, the quite low ECL emission of the biosensor incubated with 10 pMmiRNA-141 or 10 pM miRNA-155 was nearly the same as the blank one. However, the biosensor incubated with a pure agent of 1 pM target miRNA-21 or a mixture containing 1 pM target miRNA-21 presented a strikingly high ECL emission, suggesting the excellent specificity of biosensor for miRNA-21 detection. All of the results showed the eximious performance of the well-designed ECL biosensor.

Application. The analytical recovery experiment was employed to testify the practical application of the biosensor. First, different concentrations of target miRNA-21 were prepared with diluted human serum (standard addition method), which was later tested by the designed biosensor. As seen in Table 1, the recoveries of miRNA-21 samples ranged from 96.26% to 99.23% with the RSD from 0.814% to 3.174%, which showed great potential for the well-designed method in miRNA-21 detection.

To further explore the biosensor's applicative prospects, miRNA-21 in MCF-7 (human breast adenocarcinoma cancer line) and HeLa (human cervical cancer cell line) was evaluated by testing the ECL emission. As seen in Figure 6, the ECL intensity of MCF-7 cells increased apparently corresponding as the number of MCF-7 increased from 0 to 100 000 cells, suggesting the high expression of miRNA-21 in MCF-7 cells. Also, the ECL intensity of HeLa had no significant changes compared with that of blank samples even at a high concentration of 10 000 cells, which was in accordance to the low expression of miRNA-21 in HeLa cells. All of the results were aligned with the previous studies,[21,22] showing a

DOI: 10.1021/acs.analchem.9b00728
Anal. Chem. 2019, 91, 4883−4888

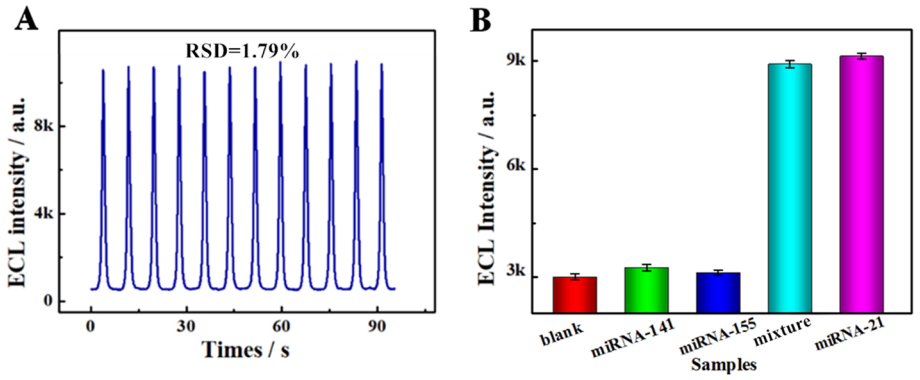

Figure 5. (A) Stability of the ECL biosensor with 10 pM miRNA-21 under 16 cycles scanning. (B) Selectivity of the ECL biosensor toward target miRNA-21 detection (blank, 10 pMmiRNA-141, 10 pM miRNA-155, 1 pM target miRNA-21, and a mixture of 10 pM miRNA-141, 10 pM miRNA-155, and 1 pM target miRNA-21).

Table 1. Recovery Experiment of miRNA-21

actual concentration (pM)	found concentration (pM)	recovery (%)	RSD (%)
0.01	0.009828	98.28	3.174
0.1	0.09626	96.26	1.672
1	0.9874	98.74	3.171
10	9.923	99.23	0.814

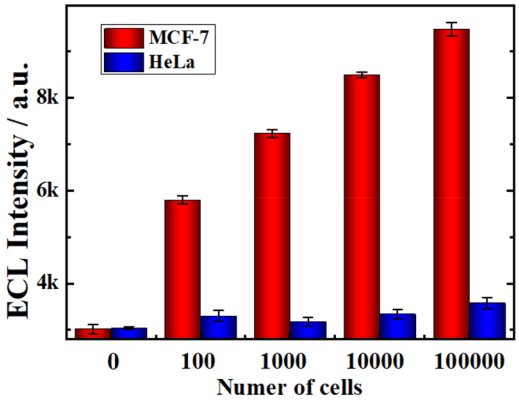

Figure 6. ECL response of the designed biosensor with different number of MCF-7 and HeLa cancer cell lines.

good potentiality of the designed biosensor in ultrasensitive detection of miRNA from cancer cells.

CONCLUSIONS

In conclusion, we proposed a novel ECL biosensor based on a Zn^{2+}-driven DNA rolling machine for speedy ultrasensitive detection of miRNA. First, the originally designed DNA rolling machine simply assembled by a large number of leg DNA attracted on the AuNP provided a high local concentration of leg DNA matched with track DNA, which not only overcame the derailing of leg DNA but also changed the motion mode from step-by-step walking to high-speed rolling to overcome the shortages of traditional DNA walking machines. Second, for improving the sensitivity of the biosensor, a finite amount of target miRNA was transformed into a large amount of Zn^{2+} by dissolving ZnO, which surmounted the weakness of common target amplification methods including enzyme cleavage and polymerization. Most importantly, with the outstanding performance of sensitivity and stability, especially for high-speed moving, the biosensor paved a prospective way for application in clinical analyses and rapid diagnosis.

ASSOCIATED CONTENT

Supporting Information

The Supporting Information is available free of charge on the ACS Publications website at DOI: 10.1021/acs.analchem.9b00728.

Reagents and materials; apparatus, preparation of nanocomposites, material characterization, and comparison of different methods for miRNA detection (PDF)

AUTHOR INFORMATION

Corresponding Authors

*Tel.: +86-23-68252277; Fax: +86-23-68253172. E-mail: hjwang@swu.edu.cn.

*Tel.: +86-23-68252277; Fax: +86-23-68253172. E-mail: yuanruo@swu.edu.cn.

ORCID

Yaqin Chai: 0000-0003-4392-9592

Ruo Yuan: 0000-0003-3664-6236

Notes

The authors declare no competing financial interest.

ACKNOWLEDGMENTS

This work was financially supported by the National Natural Science Foundation of China (21775124, 21575116, 21804110, and 21675129), the Fundamental Research Funds for the Central Universities (XDJK2016E055), and the Chongqing Research Program of Basic Research and Frontier Technology (cstc2017jcyjA1305).

REFERENCES

(1) Li, Y. Y.; Wang, G. A.; Mason, S. D.; Yang, X. L.; Yu, Z. C.; Tang, Y. A.; Li, F. *Chem. Sci.* **2018**, *9*, 6434−6439.

(2) Ma, P. Q.; Liang, C. P.; Zhang, H. H.; Yin, B. C.; Ye, B. C. *Chem. Sci.* **2018**, *9*, 3299−3304.

(3) Liu, W.; Chen, A. Y.; Li, S. K.; Peng, K. F.; Chai, Y. Q.; Yuan, R. *Anal. Chem.* **2019**, *91*, 1516−1523.

(4) Yan, T. T.; Zhu, L. Y.; Ju, H. X.; Lei, J. P. *Anal. Chem.* **2018**, *90*, 14493−14499.

(5) Cha, T. G.; Pan, J.; Chen, H. R.; Robinson, H. N.; Li, X.; Mao, C. D.; Choi, J. H. *J. Am. Chem. Soc.* **2015**, *137*, 9429−9437.

(6) Li, N. X.; Du, M. Y.; Liu, Y. C.; Ji, X. H.; He, Z. K. *ACS Sens* **2018**, *3*, 1283−1290.

DOI: 10.1021/acs.analchem.9b00728
Anal. Chem. 2019, 91, 4883−4888

(7) Qu, X. M.; Zhu, D.; Yao, G. B.; Su, S.; Chao, J.; Liu, H. J.; Zuo, X. L.; Wang, L. H.; Shi, J. Y.; Wang, L. H.; Huang, W.; Pei, H.; Fan, C. H. *Angew. Chem., Int. Ed.* **2017**, *56*, 1855−1858.
(8) Pei, R. J.; Taylor, S. K.; Stefanovic, D.; Rudchenko, S.; Mitchell, T. E.; Stojanovic, M. N. *J. Am. Chem. Soc.* **2006**, *128*, 12693−12699.
(9) Yang, X. L.; Tang, Y. A.; Mason, S. D.; Chen, J. B.; Li, F. *ACS Nano* **2016**, *10*, 2324−2330.
(10) Giordano, R. J.; Cardo-Vila, M.; Lahdenranta, J.; Pasqualini, R.; Arap, W. *Nat. Med.* **2001**, *7*, 1249−1253.
(11) Zeng, L. W.; Zhou, D. H.; Gong, J. Y.; Liu, C. S.; Chen, J. H. *Anal. Chem.* **2019**, *91*, 1724−1727.
(12) Wang, D. F.; Vietz, C.; Schroder, T.; Acuna, G.; Lalkens, B.; Tinnefeld, P. *Nano Lett.* **2017**, *17*, 5368−5374.
(13) You, M. X.; Lyu, Y. F.; Han, D.; Qiu, L. P.; Liu, Q. L.; Chen, T.; Wu, C. C.; Peng, L.; Zhang, L. Q.; Bao, G.; Tan, W. H. *Nat. Nanotechnol.* **2017**, *12*, 453−459.
(14) Yehl, K.; Mugler, A.; Vivek, S.; Liu, Y.; Zhang, Y.; Fan, M. Z.; Weeks, E. R.; Salaita, K. *Nat. Nanotechnol.* **2016**, *11*, 184−190.
(15) Zhang, P.; Jiang, J.; Yuan, R.; Zhuo, Y.; Chai, Y. Q. *J. Am. Chem. Soc.* **2018**, *140*, 9361−9364.
(16) Xie, L. L.; Yang, X.; He, Y.; Yuan, R.; Chai, Y. Q. *ACS Appl. Mater. Interfaces* **2018**, *10*, 15200−15206.
(17) Xu, Z. Q.; Zhang, P.; Chai, Y. Q.; Wang, H. J.; Yuan, R. *Chem. Commun.* **2018**, *54*, 8741−8744.
(18) Gai, P. P.; Gu, C. C.; Li, H. Y.; Sun, X. Z.; Li, F. *Anal. Chem.* **2017**, *89*, 12293−12298.
(19) Liu, X. J.; Chen, M. Q.; Hou, T.; Wang, X. Z.; Liu, S. F.; Li, F. *Biosens. Bioelectron.* **2014**, *54*, 598−602.
(20) Radi, A.; Acero Sánchez, J. L.; Baldrich, E.; O'Sullivan, C. K. *J. Am. Chem. Soc.* **2006**, *128*, 117−124.
(21) Oudeng, G.; Au, M.; Shi, J. Y.; Wen, C. Y.; Yang, M. *ACS Appl. Mater. Interfaces* **2018**, *10*, 350−360.
(22) Guo, J.; Mingoes, C.; Qiu, X.; Hildebrandt, N. *Anal. Chem.* **2019**, *91*, 3101−3109.

DOI: 10.1021/acs.analchem.9b00728
Anal. Chem. 2019, 91, 4883−4888